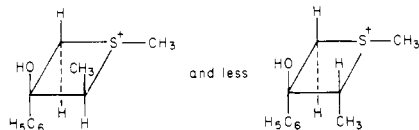
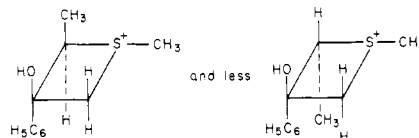


- (10) Yang, N. C.; Yang, D. H. *J. Am. Chem. Soc.* **1958**, *80*, 2913.  
Yang, N. C.; Morduchowitz, A.; Yang, D. H. *Ibid.* **1963**, *85*, 1017.  
(11) Yates, P.; Szabo, A. G. *Tetrahedron Lett.* **1965**, 485.  
(12) Ylides X and XI can also undergo prototropic rearrangement as shown in eq 9 to shift the carbon-sulfur double bond to the position  $\alpha$  to the carbonyl. However, reaction of these new ylides with  $\text{HBF}_4$  would also be expected to give sulfonium salts (VII and VIII).  
(13) On the basis of minimization of steric hindrance, photolysis of VII would be expected to give mainly



and photolysis of VIII mainly



- (14) Gould, E. S. "Mechanism and Structure in Organic Chemistry"; Holt, Reinhart and Winston: New York, 1959; p 220.  
(15) Turro, N. J. "Modern Molecular Photochemistry"; Benjamin Cummings Publishing Co.: Menlo Park, 1978; p 384.  
(16) Huyser, E. S.; Neckers, D. C. *J. Am. Chem. Soc.* **1963**, *85*, 3641.  
(17) Ireland, J. F.; Wyatt, P. A. H. *Adv. Phys. Org. Chem.* **1968**, *12*, 188.  
(18) Darwish, D.; Hui, S. H.; Tomilson, R. *J. Am. Chem. Soc.* **1968**, *90*, 5631.  
(19) Scartazzini, R.; Mislow, K. *Tetrahedron Lett.* **1967**, 2719.  
(20) Crivello, J. V.; Lam, J. H. W. *J. Polym. Sci., Polym. Chem. Ed.* **1979**, *17*, 977.

## Structure-Property Relationships of Polyacetylene/Polybutadiene Blends

Michael F. Rubner,\* Sukant K. Tripathy, Jacque Georger, Jr., and Patricia Cholewa

GTE Laboratories, Inc., Waltham, Massachusetts 02254. Received August 27, 1982

**ABSTRACT:** Polymer blends of polyacetylene and *cis*-1,4-polybutadiene of various compositions were prepared and examined. The resulting blends were characterized by infrared spectroscopy, thermal analysis, and X-ray diffraction techniques. The blends were found to exist as two-phase systems consisting of crystalline polyacetylene and amorphous polybutadiene. The mechanical properties of the blends were found to be a function of the blend composition, with low polyacetylene compositions exhibiting rubbery elastic properties and high polyacetylene compositions behaving more plastic-like. Doping the blends with electron acceptors such as iodine and ferric chloride resulted in electrical conductivities in the 10–100  $\Omega^{-1} \text{cm}^{-1}$  range. For blends containing 40–60% polyacetylene, the conductivity could be further enhanced by stretching the blend prior to doping. Results suggest that this phenomenon is a complex process of stress-induced ordering that is taking place in the polyacetylene phase. Varying the composition of the blend allowed a range of mechanical and electrical properties to be obtained that thus extend the useful properties of polyacetylene.

### Introduction

Polyacetylene has been the subject of many recent research activities. This is primarily due to the unique electrical properties manifested by polyacetylene when it is exposed to electron-donating or electron-withdrawing dopants.<sup>1</sup> Typically, polyacetylene is prepared in the form of a film or as a powder. However, the material is insoluble, intractable, and infusible, and, although reasonable mechanical properties are observed<sup>2</sup> when it is maintained in an inert atmosphere, upon exposure to ambient conditions, polyacetylene quickly becomes brittle. For these reasons, morphological modification of polyacetylene and its characterization have been difficult. Additionally, lack of processibility and stability are the major stumbling blocks in finding suitable applications for this fascinating material.

Attempts have been made to improve the undesirable mechanical properties without compromising the electrical properties via synthetic techniques. For example, copolymers of polyacetylene with phenylacetylene<sup>3</sup> and methylacetylene<sup>4</sup> have been prepared and characterized. This was carried out with the hope that while the unchanged structure of the polymer backbone will result in unaltered electrical properties, the side groups will impart the required processing advantage. The resultant materials were indeed found to have some processing advantages (soluble copolymers can be obtained with phenylacetylene) over the homopolymer; however, this was accomplished

only with significant decrease in the electrical conductivity. While this behavior is not well understood, it is speculated that the electrical properties are very sensitive to the arrangement of chains and order in the polymeric "microdomains".<sup>5</sup> Interestingly, Galvin and Wnek recently reported<sup>6</sup> that films consisting of polyacetylene blended with polyethylene remained tough and flexible after prolonged exposure to air. Yet the films could be doped to conductivities of about 10  $\Omega^{-1} \text{cm}^{-1}$ . Obviously, a detailed study of polyblends can make a significant impact on the understanding of the nature of electrical transport in these materials and the structural requirements thereof.

In our laboratory we are presently carrying out these investigations with the polyblends of polyacetylene with an elastomer. In this paper we report on polyblends in which the elastomeric component is *cis*-1,4-polybutadiene. The selection of an elastomer as a component of the blend can be rationalized at two levels. First, the contrast between the rubbery nature of polybutadiene and the polycrystalline nature of polyacetylene can be exploited to gain information on morphology, structure, and the physical properties of the blend. Also, by blending with a flexible polymer having a low  $T_g$ , a full range of blend compositions can be obtained. Second, the excellent mechanical properties of polyblends containing a rubbery component are well-known, and therefore a similar enhancement of properties would be expected in the case of a polyacetylene blend. In other words, polyacetylene/elastomer blends not

only present an opportunity to gain an understanding of the requisite structural features for high conduction but also open up avenues for morphological modifications and hence variations in electrical and mechanical properties through physicochemical means.

### Experimental Section

**Materials.** All solvents were dried and distilled under argon. Acetylene was bubbled through a glass-packed sulfuric acid tower followed by passage through a KOH/3-Å molecular sieve column and a cold trap (dry ice/acetone cooled) prior to use. The  $\text{Ti}(\text{OBu})_4/\text{Et}_3\text{Al}$  Ziegler-type catalyst was prepared according to the methods of Ito et al.<sup>7</sup> The stock catalyst mixture consisted of 1.7 mL of  $\text{Ti}(\text{OBu})_4$  and 2.7 mL of  $\text{Et}_3\text{Al}$  in 20 mL of toluene. *cis*-1,4-Polybutadiene (98%) was used as received (Scientific Polymer Products, Inc.); average MW = 200 000–300 000. Iodine, ferric chloride, and lithium perchlorate were used as received. All manipulations were carried out by using vacuum line techniques or in an inert atmosphere.

**Experimental Methods.** Polyacetylene blends were prepared in the following manner. In a typical experiment, 2.5 g of polybutadiene was dissolved in 25 mL of toluene. Next, a predetermined amount of the stock catalyst was added to the solution (usually 1–5 mL). After the solution was thoroughly mixed, the reaction vessel was placed under dynamic vacuum to remove the toluene. This results in a uniform coating on the walls of the reaction vessel consisting of polybutadiene impregnated with the catalyst. The vessel was then cooled to  $-78^\circ\text{C}$  (using a dry ice/acetone bath) followed by the introduction of acetylene gas to a pressure of 1 atm. As the polymerization proceeds, the light brown coating turns to a shiny gold-black film. The final composition of the blend is a function of the exposure time to acetylene gas and the amount of catalyst added to the elastomer. Once prepared, the resultant blend was washed with cold ( $-78^\circ\text{C}$ ) heptane and dried at  $10^{-3}$  torr for 8 h.

The composition of the blend was estimated by elemental analysis and instrumental techniques such as FT IR, DSC, and X-ray diffraction. The various procedures used to dope the blends have been described in previous publications.<sup>8</sup>

**Characterization of the Blends.** Infrared spectra were recorded on a Nicolet 3600E Fourier transform infrared spectrophotometer (FT IR) using an ATR (attenuated total reflectance) attachment. X-ray diffraction patterns were recorded on a Phillips vertical diffractometer with a solid-state scintillation detector ( $\text{Cu K}\alpha$  radiation). Differential thermal analysis (DSC) was performed with a DuPont 1090 thermal analyzer and a DSC module. The melting point,  $T_m$ , and crystallization point,  $T_c$ , were taken as the maxima in the endothermic and exothermic peaks, respectively. Glass transition temperatures ( $T_g$ ) were determined by using the intersection method. DC conductivities were measured by using standard four-point probe techniques. Stress-strain curves were obtained on an Instron machine at a strain rate of  $0.05\text{ min}^{-1}$ . Sample dimensions were typically  $0.35\text{ cm}$  wide and  $0.01\text{ cm}$  thick. Some samples were stretched with a homemade bench-top machine capable of operating at a constant strain rate. In both cases, the samples were stretched in an ambient atmosphere.

### Results and Discussion

**Blend Structure.** The X-ray diffraction patterns of various compositions of polyacetylene/polybutadiene (PA/PB) blends are shown in Figure 1. There are two main features apparent in these scans. First, there is a broad amorphous halo centered about  $2\theta = 19.8^\circ$  characteristic of amorphous PB. The second feature is a narrow, relatively sharp diffraction peak centered at  $2\theta = 23\text{--}24^\circ$ , which is the main interchain reflection (110) of crystalline *cis*-PA.<sup>9</sup> As can be seen, the relative intensities of these two peaks depend upon the composition of the blend, and the diffraction patterns appear to be a superposition of the two blend components. This simple superposition of the two diffraction patterns clearly indicates the blend to be at least a two-phase system, with distinct domains of polyacetylene (polycrystalline) and polybutadiene. Similar conclusions can be made from electron diffraction studies

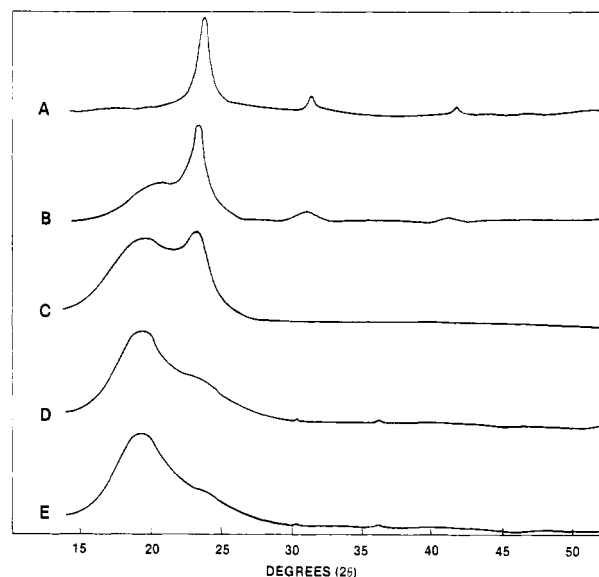


**Figure 1.** X-ray diffraction patterns of PA/PB blends: (A) 100/0; (B) 85/15; (C) 60/40; (D) 15/85; (E) 0/100.

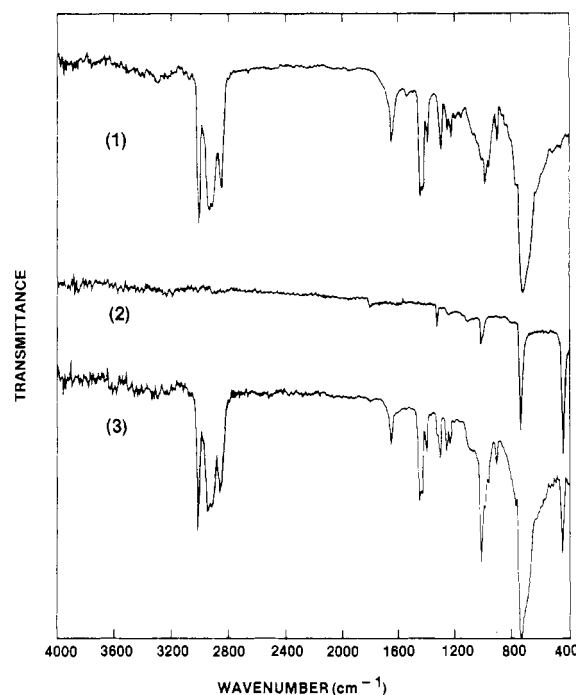


**Figure 2.** Infrared spectra of (1) *cis*-1,4-polybutadiene, (2) *cis*-polyacetylene, and (3) a 40/60 PA/PB blend.

of fractured specimens, and since the composite electron diffraction pattern was obtained with a 5000-Å selected-area aperture, this indicates a homogeneous distribution of phases, at least at this scale. Analysis of the (110) peak of polyacetylene reveals that there is a small amount of line broadening ( $1.2\text{--}3.0^\circ$ ) as the PB content of the blend increases. This indicates that the presence of PB during the polymerization of PA affects the size and/or perfection of the PA crystallites. The extent of this phenomenon, however, can only be estimated (measuring the full width at half-maximum and assuming a symmetrical reflection geometry) due to the strong overlap of the PB and PA reflections.

Figure 2 shows the infrared spectra of (1) *cis*-1,4-polybutadiene, (2) *cis*-polyacetylene, and (3) a 40/60 (PA/PB) blend. The spectrum of the blend is a simple superposition of the spectra of the two blend components, with no observable frequency shifts in the absorption bands. The

Table I  
Thermal Transitions of PB in PA/PB Blends as a Function of Blend Composition

PA/PB composition	$T_g, ^\circ\text{C}$	$T_c, ^\circ\text{C}$	$T_m, ^\circ\text{C}$
0/100	-104	-70	-5
15/85	-104	-73	-16
40/60	-106	-69	-19
60/40	-104	-70	-19
85/15	-105	-68	-27

<sup>a</sup>  $T_g$ ,  $T_c$ , and  $T_m$  are the glass transition temperature, crystallization temperature, and melting temperature, respectively, of the PB phase in the PA/PB blend.

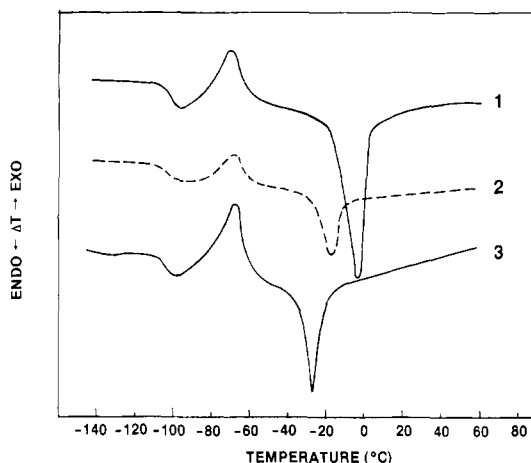


Figure 3. Differential thermograms (DSC's) of (1) *cis*-1,4-polybutadiene, (2) a 40/60 PA/PB blend, and (3) an 85/15 PA/PB blend.

increase in the intensity of the absorption band at  $1015\text{ cm}^{-1}$  indicates that the blend contains some of the *trans* isomer of PA. Band assignments for PA and PB have been reported in literature.<sup>10</sup> For blends with compositions either higher or lower in PA content, the infrared spectrum is dominated by the absorption bands of the major component. The infrared results in conjunction with the X-ray diffraction and electron diffraction studies present a persuasive argument against the presence of any "mixed phases". It should be mentioned here, however, that repeated washing of the blend by toluene did not remove 100% of the elastomeric phase. This can be attributed to physical entanglement, and yet presence of a few cross-links between the polybutadiene and polyacetylene chains cannot be ruled out. Since the polymerization of acetylene was carried out in a solid solution of the elastomer, the elastomer is believed to be a continuous phase for all blend compositions. There are strong indications that at high PA compositions (>40%), the PA phase is also continuous or quasi-continuous. On the other hand, below the  $\approx 40\%$  PA composition, the PA phase consists primarily of discontinuous domains.

**Thermal Properties.** Information about the compatibility of polymer blends can be obtained by detection of changes in the glass transition temperatures ( $T_g$ ) of one or more of the blend components. For example, when the two components of the polymer blend exist as distinct phases (incompatible), the  $T_g$ 's of the components remain identical in temperature and width with those of the unblended components.<sup>11</sup> This is the case in PA/PB blends, where it was found that the  $T_g$  of PB remains unchanged throughout the range of compositions examined. Figure 3 is a sample of the DSC thermograms obtained for various compositions of PA/PB blends. It is interesting to note, however, that although the  $T_g$  of PB remains unchanged

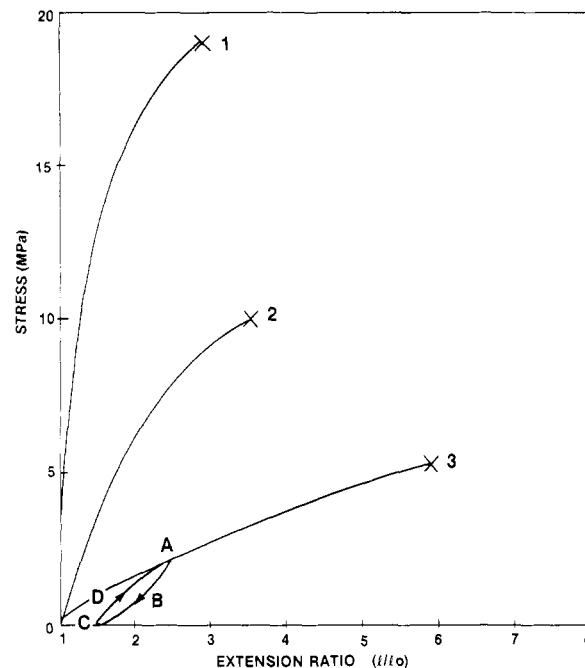


Figure 4. Stress-strain curves for (1) an 85/15 PA/PB blend, (2) a 60/40 PA/PB blend, and (3) a 15/85 PA/PB blend. Curve ABCD shows the effect of unloading and reloading the stress on a PA/PB blend.

Table II  
Mechanical Properties of PA/PB Blends as a Function of Blend Composition

PA/PB composition	tensile strength, MPa	Young's modulus, MPa	$L/L_0^a$
100/0 <sup>b</sup>	21	200	1.8
85/15	19	125	2.8
40/60	10	22	3.5
15/85	5	2	5.8

<sup>a</sup> Extension ratio at break. <sup>b</sup> From ref 2.

in the blends, the melting point ( $T_m$ ) of PB was observed to decrease with increasing PA content. Melting point depressions are frequently encountered in compatible blends,<sup>11</sup> but they are less common in incompatible blends. The  $T_m$  depression reflects the effect PA has on reducing the size or perfection of PB crystallites. This is not surprising, considering that pure *cis*-PB crystallizes only with difficulty and therefore is highly susceptible to diluent effects. In this case, polyacetylene forms a distinct phase that is uniformly dispersed, and its typical physical dimensions are approximately submicron (electron microscopy<sup>12</sup>). In this light, a pronounced diluent effect is not surprising. Although not shown in Figure 3, when the PA/PB blends are heated to  $200^\circ\text{C}$ , isomerization of *cis*-PA to *trans*-PA occurs as is evident by the presence of an exothermic peak centered at  $135^\circ\text{C}$ .

**Mechanical Properties.** The stress-strain properties of PA/PB blends of various compositions are shown in Figure 4. Predictably, as the percentage of the crystalline PA phase is increased in the blend, the tensile strength increases and the maximum extension ratio ( $L/L_0$ , where  $L_0$  is the starting length and  $L$  is the final length) is lowered. This is an example of an amorphous elastomer that has been embedded with microcrystalline domains. These domains serve as physical cross-links that impart stiffness to the material by reducing the mobility of the elastomeric domains.

Table II lists some of the mechanical properties of PA/PB blends. Young's modulus was estimated by the

Table III  
Electrical Conductivity and Dopant Uptake of PA/PB Blends as a Function of Blend Composition and Mechanical Treatment

	PA/PB composition	dopant	max wt % dopant uptake	conductivity, $\Omega^{-1} \text{cm}^{-1}$
1.	100/0	iodine	240	200-500
2.	85/15	iodine	136	80
3.	60/40	iodine	40	4
4.	40/60	iodine	35	15
5.	15/85	iodine	150	10
6.	60/40	$\text{FeCl}_3$	16	116
7.	85/15	$\text{LiClO}_4$	no data	1.0 <sup>a</sup>
8.	40/60 (1)	iodine	35	15
	(2)	iodine	91	575 <sup>b</sup>
9.	40/60 (1)	iodine	23	4
	(2)	iodine	19	50 <sup>c</sup>
10.	60/40 (1)	iodine	35	4
	(2)	iodine	43	26 <sup>d</sup>

<sup>a</sup> Electrochemically doped. <sup>b</sup> Stretched before doping ( $L/L_0 = 6.0$ ). <sup>c</sup> Stretched before doping ( $L/L_0 = 4.2$ ).

<sup>d</sup> Stretched before doping ( $L/L_0 = 3.0$ ).

method described by Druy et al.<sup>2</sup> in which the elastic region is determined by unloading and reloading samples under stress. An example of an elastic hysteresis loop generated by this method is shown in curve 3 of Figure 4. The elastic range decreased as the PA content increased, and at high PA levels (greater than  $\approx 40\%$ ), the samples underwent almost complete plastic deformation. This is a result of the rigidity that is imposed on the system by the crystalline PA regions. Thus, by varying the composition of the blend, a range of mechanical properties can be obtained which, when combined with the unique electrical properties of doped PA, provides materials that are tough, flexible, and electrically conductive (see next section).

It has been reported<sup>2</sup> that in order to reach the maximum extension ratio in *cis*-PA ( $L/L_0 = 3.3$ ), it is important that the sample not be exposed to air at any time. Also, when PA is exposed to air, the material becomes brittle within a few hours and cannot be mechanically stretched. PA/PB blends, on the other hand, depending upon their composition, retain their mechanical properties on air exposure, and the maximum extension at break remains unchanged even after exposure to air for 2 h. The mechanical stability of PA/PB blends, as noted above, depends on the composition of the blend. For example, blends with greater than  $\approx 30\%$  PA become brittle in air after a few days, whereas blends with less than  $\approx 30\%$  PA retain good mechanical properties for weeks. The reactivity of the isolated double bonds in PB, combined with the poor oxygen barrier provided by the PB matrix, precludes any long-range stability in these materials. However, results on blends of PA and triblock polymers such as polystyrene/polybutadiene/polystyrene<sup>12</sup> and results reported on PA blended with polyethylene<sup>6</sup> indicate that there is a possibility of achieving long-range mechanical stability in PA blends.

**Electrical Properties.** The electrical conductivity of PA/PB blends increases dramatically upon exposure to suitable dopants. Table III lists the maximum level of conductivity achieved for the blend compositions that were investigated. Unless otherwise noted, all of the blends were doped by solution doping techniques.<sup>8</sup> High levels of conductivity could be obtained with iodine (doped 2-3 h) or  $\text{FeCl}_3$  (doped 24 h) as the dopant or, alternatively, the blends could be electrochemically doped with a 0.3 M solution of  $\text{LiClO}_4$  at a constant potential of +3.9 V vs. a  $\text{Li/Li}^+$  reference electrode. The amount of dopant uptake

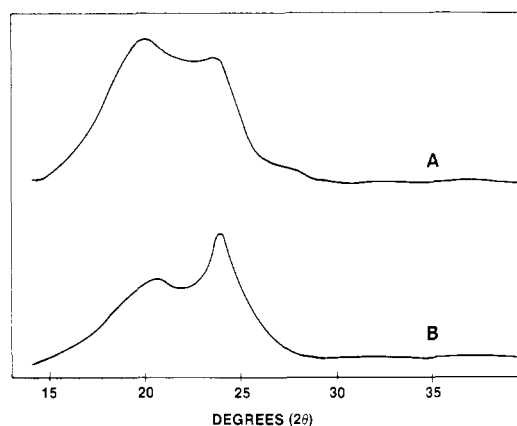


Figure 5. X-ray diffraction patterns of a 40/60 PA/PB blend (a) prior to stretching and (b) after stretching ( $L/L_0 = 6.0$ ).

(weight percent) increased as the composition of PA in the blend increased. However, a deviation from this trend was observed in the 15% PA blend (Table III, no. 5), which picked up 150 wt % iodine. In this case, the excess iodine that is normally removed during the washing step remained trapped in the PB phase and therefore contributed to the final weight. Any iodine remaining in the PB phase should not appreciably influence the electrical properties of the blend (pure PB is not rendered electrically conductive when exposed to iodine). Also, there was no evidence of iodine clusters in either the PB or PA phase as indicated by TEM.<sup>12</sup> The reaction of iodine with the isolated double bonds in PB, however, cannot be ruled out.

The conductivity of PA/PB blends with compositions in the 40-60% PA range could be further enhanced by first stretching the blend and then exposing it to a dopant. For example, the most dramatic results were obtained with a 40/60 PA/PB blend (Table III, no. 8), in which the conductivity increased from  $15 \Omega^{-1} \text{cm}^{-1}$  for the unstretched material to  $575 \Omega^{-1} \text{cm}^{-1}$  for the material stretched prior to doping. Blends outside of this compositional range generally showed no difference in conductivity after stretching and subsequent doping. The magnitude of the change in conductivity resulting from stretching the blends prior to doping was related to the extension ratio ( $L/L_0$ ), with the greatest changes occurring in samples that reached the highest ratio.

The blends that exhibited stretch-enhanced conductivity had two things in common. First, stretching resulted in complete plastic deformation of the sample, and second, the X-ray diffraction scan of the stretched material was different from that of the unstretched material. For example, Figure 5 shows the diffraction scans for the 40/60 PA/PB blend before stretching (A) and after stretching (B). In this case, the extension ratio of the blend was  $L/L_0 = 6$ . As indicated by Figure 5, there has been a change in the relative intensities of the two main diffraction peaks. The peak earlier described as the interchain reflection of crystalline *cis*-PA ( $2\theta = 23.9^\circ$ ) has increased in intensity (total integrated area) relative to the amorphous halo of PB. Additionally, no detectable change was observed in the infrared spectra of the blends subsequent to stretching, thus indicating that the composition of the blend was unchanged.

This suggests that there has been an increase in the crystallinity in the PA regions, possibly resulting from the partial orientation of the polyacetylene domains. It has been reported that stretch elongation of fibrillar PA leads to significant improvement in the electrical conductivity.<sup>13</sup> In this case, partial orientation of the fibers found in PA films prepared with the Shirakawa catalyst resulted in

strong electrical and optical anisotropy.<sup>14</sup> The polyacetylene component in the PA/PB blends, on the other hand, does not have a fibrillar morphology,<sup>12</sup> and it is therefore difficult to make an analogous statement about stretch-elongated blends. One possible explanation is that the degree of crystallinity and extent of order in the normally intractable PA phase has been improved as a result of stretching. This may be the first example where increased order in PA was accomplished by purely physical means.

We speculate that in the 40–60% compositional range, both PA and PB form continuous or quasi-continuous phases that are in intimate contact with each other (vide thermal data). Upon stretching, the stress is directly transferred to the PA domains which are subsequently stretch oriented, deforming the PB matrix in tandem (which results in complete plastic deformation). Thus, a complex process of stress-induced ordering is taking place in the PA phase, where the dominant morphology is a lamellar polycrystalline arrangement.<sup>12</sup> We cannot ascertain at this stage whether the improved order is a result of the stretch orientation of amorphous PA or if it is a complete deformation of the crystalline phase and subsequent crystallization. In either case, it is difficult to comprehend such behavior in light of the fact that PA is such an intractable material. The fact that improved order occurs in the blend upon stretching, however, attests to the hypothesis that the PB matrix forms the right elastomeric template to allow extensive stretching of the PA phase before its yield point is reached (Table III). In the case of fibrillar PA, stretching only results in alignment of the fibrils, and no reorganization of the fibrils could be expected due to the limited extension ratios achieved. In order to fully understand this phenomenon, it will be necessary to investigate any optical and electrical anisotropy properties of stretched blends and also the effect of phase distribution. In the latter case, preliminary results indicate that the size of the PA domains, which is in part controlled by the amount of stock catalyst added to the PB, also has a major impact on the magnitude of the stretch-enhancement of the conductivity. All of these issues are the subject of continuing investigation in this laboratory. Detailed results of electron microscopy studies on this and other PA/elastomer blend systems will be reported in a subsequent publication.<sup>12</sup>

In our previous work,<sup>8a</sup> we have shown that there is a relationship between the degree of crystallinity of PA and the level of conductivity obtained after doping. The most crystalline materials were found to reach the highest levels of conductivity ( $>50 \Omega^{-1} \text{ cm}^{-1}$ ), whereas materials containing a significant amorphous fraction could only be doped to conductivities of about  $10^{-3} \Omega^{-1} \text{ cm}^{-1}$ . The degree of line broadening (110 peak) varied in the materials that reached high conductivity ( $1\text{--}5^\circ$ ); however, it could not be directly related to the conductivity level reached upon doping. These observations, combined with our results on PA/PB blends, support the conjecture that the level of crystallinity in PA influences the level of conductivity reached after doping and that high levels of conductivity can only be achieved with crystalline PA. In other words, more ordered microdomains dope to higher levels of conductivity. Thus, high conductivities in the bulk can occur if a suitable low-resistance pathway is established interconnecting the domains.

The conductivity of the doped blends remained essentially constant throughout the bulk of the material. For example, if the surface layers of a thick film of the blend were successively removed and the conductivity subse-

quently measured, no significant difference in the conductivity was observed. In some cases, however, a surface skin of PB was deposited during the washing procedure which conducted less readily than the interior of the sample. This skin could be easily removed by scraping of the surface, which then revealed the true electrical properties of the bulk of the material.

The stability of the conductivity of doped PA was not improved in the PA/PB blends. For example, a 60/40 PA/PB blend (iodine doped) exposed to ambient conditions for 4 months dropped from a conductivity of  $25 \Omega^{-1} \text{ cm}^{-1}$  to  $10^{-1} \Omega^{-1} \text{ cm}^{-1}$ . This is partly due to the poor diffusion barrier properties that elastomers such as PB have against oxygen and moisture. Similar results were obtained with other blend compositions.

## Summary

When PA is polymerized in the presence of PB, an incompatible blend consisting of an amorphous PB phase and crystalline PA phase is formed. Results from infrared and thermal analysis and electron microscopic and X-ray diffraction studies are consistent with the above description of a two-phase system. The presence of PA in the blend, however, does interfere with the crystallization of PB, resulting in a large melting point depression in blends with a high PA content.

The mechanical properties of the blend are a function of the blend composition, with low PA compositions exhibiting rubbery elastic properties (low tensile strength and reversible strain) and high PA compositions behaving more plastic-like (high tensile strength and plastic strain). In all cases, tough flexible films are obtained that maintain their mechanical integrity (composition dependent) for weeks upon exposure to air.

PA/PB blends can be doped with electron acceptors, such as iodine, to reach conductivities in the  $10\text{--}100 \Omega^{-1} \text{ cm}^{-1}$  range. Further increases in conductivity can be obtained in blends containing 40–60% PA by stretching the blend prior to doping. In this case, conductivities as high as  $575 \Omega^{-1} \text{ cm}^{-1}$  could be achieved. We speculate that this is, in part, a result of stress-induced order in the PA domains.

In conclusion, polyblends that contain PA as a component offer a wide range of mechanical and electrical properties that were heretofore not possible in conducting polymers that have been examined to date.

**Acknowledgment.** We thank Professor Gary Wnek of MIT for initiating our interest on polyacetylene blends. Enthusiastic support and valuable discussion with Dr. Peter Cukor and members of the Polymer Science group at ATL are acknowledged. We are also grateful to Mark Druy for electrochemical measurements, to Jack Ramsey for mechanical property studies, and to Mike Downey, Tom Emma, Frank Kochanek, Paul Martakos, and Kim Ostreicher for analytical support.

**Registry No.** Polyacetylene, 25067-58-7; iodine, 7553-56-2; iron trichloride, 7705-08-0; lithium perchlorate, 7791-03-9.

## References and Notes

- (1) See, e.g.: MacDiarmid, A. G.; Heeger, A. J. *Synth. Met.* **1980**, *1*, 101.
- (2) Druy, M. A.; Tsang, C. H.; Brown, N.; Heeger, A. J.; MacDiarmid, A. G. *J. Polym. Sci., Polym. Phys. Ed.* **1980**, *18*, 429.
- (3) Deits, W.; Cukor, P.; Rubner, M.; Jopson, H. *Synth. Met.* **1982**, *4*, 199.
- (4) Chien, J. C. W.; Wnek, G. E.; Karasz, F. E.; Hirsch, J. A. *Macromolecules* **1981**, *14*, 479.
- (5) Tripathy, S. K.; Kitchen, D.; Druy, M. A. *Macromolecules* **1983**, *16*, 190.
- (6) Galvin, M. E.; Wnek, G. E. *Polymer* **1982**, *23*, 795.

- (7) Ito, T.; Shirakawa, H.; Ikeda, S. *J. Polym. Chem. Polym. Chem. Ed.* 1974, 12, 11.
- (8) (a) Deits, W.; Cukor, P.; Rubner, M.; Jopson, H. *J. Electron. Mater.* 1981, 10, 683. (b) Sichel, E. K.; Knowles, M.; Rubner, M.; Georger, J., Jr. *Phys. Rev. B* 1982, 25, 5574.
- (9) Baughman, R. H.; Hsu, S. L.; Pez, G. P.; Signorelli, A. J. *J. Chem. Phys.* 1978, 68, 5405.
- (10) For polyacetylene, see: Shirakawa, H.; Ikeda, S. *Polym. J.* 1971, 2, 231. For polybutadiene, see: Haslam, J.; Willis, H. A. "Identification and Analysis of Plastics"; Van Nostrand: Princeton, NJ, 1965.
- (11) Paul, D. R.; Newman, S. "Polymer Blends"; Academic Press: New York, 1978.
- (12) Results to be published.
- (13) Park, Y. M.; Druy, M. A.; Chiang, C. K.; MacDiarmid, A. G.; Heeger, A. J.; Shirakawa, H.; Ikeda, S. *J. Polym. Sci., Polym. Lett. Ed.* 1979, 17, 195.
- (14) Fincher, C. R., Jr.; Peebles, D. L.; Heeger, A. J.; Druy, M. A.; Matsamura, Y.; MacDiarmid, A. G.; Shirakawa, H.; Ikeda, S. *Solid State Commun.* 1978, 27, 489.

## Order in Nematic Phase of Semiflexible Polymers

Gilles Sigaud<sup>†</sup> and Do Y. Yoon\*

IBM Research Laboratory, San Jose, California 95193

Anselm C. Griffin

Department of Chemistry, University of Southern Mississippi,  
Hattiesburg, Mississippi 39401. Received July 13, 1982

**ABSTRACT:** Orientational order in the nematic phase of the thermotropic aromatic polyester  $(C_{10}H_{20}OC_6H_4COOC_6H_4OC_{10}H_{20}OC_6H_4OOC_6H_4O)_x$  has been evaluated from magnetic susceptibility measurements and has been compared with those for the corresponding monomer and dimer, i.e.,  $C_6H_{11}O-C_6H_4COOC_6H_4OC_6H_{11}$  and  $C_6H_{11}OC_6H_4COOC_6H_4OC_{10}H_{20}OC_6H_4OOC_6H_4OC_6H_{11}$ , respectively. The (orientational) order parameter of this polymer near the isotropic-nematic transition is found to be ca. 0.6, compared to the corresponding order parameters of ca. 0.4 for the monomer and ca. 0.5 for the dimer. These results are thus confirmatory of the recent theory of Ronca and Yoon, which predicts that the isotropic-nematic phase transition of semiflexible polymers does not entail a very high degree of order in the resultant nematic phase and that this nematic phase should become a thermodynamically viable state for polymers with limited flexibility. This finding is contrary to the ideas of polymer crystallization or glass transition advocated on the physical impossibility of random chains with limited flexibility to fill the space.

### Introduction

The state of intermediate order, i.e., the nematic phase, of bulk polymers has been the subject of intense investigations in recent years from both experimental<sup>1-6</sup> and theoretical<sup>7,8</sup> standpoints. Although the discovery of the nematic phase of bulk polymers was rather recent, first by Roviello and Sirigue in 1975,<sup>1</sup> a large number of polymers have since been synthesized to exhibit nematic melts, and some of them are found to undergo isotropic-nematic phase transitions involving latent heat. Nematic polymers, upon processing, exhibit better chain orientation and improved mechanical properties than conventional polymers and, hence, are of great technological interest.<sup>2</sup>

From a fundamental theoretical point of view, the appearance of the nematic phase of bulk polymers present a new and challenging situation. The isotropic phase of bulk polymers wherein the polymer chains adopt *unperturbed random coil* configurations is now well established<sup>9,10</sup> in accordance with the predictions of the lattice theory of Flory.<sup>11</sup> However, in this theory the isotropic phase of random coils is predicated on the conditions that the polymer chains are sufficiently flexible. Thus, as the chain flexibility decreases, say with decreasing temperature, the isotropic phase of bulk polymers should become untenable.<sup>7,12</sup> The consequence of such limited flexibility, or semiflexibility, of random chains has been theorized to lead to a perfectly ordered state, i.e., crystalline order,<sup>12,13</sup> or glass transition,<sup>14</sup> when the crystalline order is inhibited, due to the vanishing configurational entropy of random chains. This is shown schematically in Figure 1 in terms

of relative free energy of the isotropic phase vs. temperature, wherein  $T_c$  and  $T_g$  ( $T_g$ ) denote the temperatures of crystallization<sup>12</sup> and glass transition<sup>14</sup> thus predicted.

In these theories, however, the state of intermediate order has not been considered. The possibility that the untenability of the isotropic phase of semiflexible polymers will result in a first-order transition to an ordered state was recognized early by Flory.<sup>12</sup> But it is only very recently that a detailed theory of nematic systems of semiflexible polymers was developed by Ronca and Yoon.<sup>8</sup> According to this theory, the consequence of this limited flexibility of bulk polymers should lead to the transition of the isotropic phase into a nematic phase containing considerable disorder. This is shown schematically in Figure 1 by the intersection of the free energy curve of the nematic phase with that of the isotropic phase. Therefore, the degree of conformational and orientational order in the nematic phase thus formed is predicted to be not very high, with the orientational order parameters at the transition falling in the range 0.4-0.7.

It is the intent of this paper to test the basic premise of this theory of Ronca and Yoon that the isotropic-nematic transition of semiflexible polymers does not entail a very high degree of orientational order in the resultant nematic phase. The subject of conformational order is touched upon only briefly here and will be discussed in detail in a separate paper.<sup>15</sup>

For this purpose we chose the thermotropic polyester  $(C_{10}H_{20}OC_6H_4COOC_6H_4OC_{10}H_{20}OC_6H_4OOC_6H_4O)_x$  (I), shown schematically in Figure 2a, because of its relatively low isotropic-nematic transition temperature  $T_{NI} \approx 215^\circ\text{C}$  and the resultant thermal stability of the polymer in the nematic state. A detailed study of the thermal properties of this class of thermotropic polymers and the

<sup>†</sup> IBM World Trade Postdoctoral Fellow. Permanent address: Centre de Recherche Paul Pascal Domaine Universitaire, 33405 Talence, France.